YIELD-DRIVEN ELECTROMAGNETIC OPTIMIZATION VIA MULTILEVEL MULTIDIMENSIONAL MODELS

J.W. Bandler, R.M. Biernacki, S.H. Chen
P.A. Grobelny and S. Ye

SOS-93-8-R

March 1993

YIELD-DRIVEN ELECTROMAGNETIC OPTIMIZATION VIA MULTILEVEL MULTIDIMENSIONAL MODELS

John W. Bandler, Fellow, IEEE, Radoslaw M. Biernacki, Senior Member IEEE, Shao Hua Chen, Member, IEEE, Piotr A. Grobelny and Shen Ye, Member, IEEE

Abstract

We present the foundation of a sophisticated hierarchical multidimensional response surface modeling system for efficient yield-driven design. Our scheme dynamically integrates models and data base updating in real optimization time. The method facilitates a seamless, smart optimization-ready interface. It has been specially designed to handle circuits containing complex subcircuits or components whose simulation requires significant computational effort. This approach makes it possible, for the first time, to perform direct gradient-based yield optimization of circuits with components or subcircuits simulated by an electromagnetic simulator. The efficiency and accuracy of our technique are demonstrated by yield optimization of a three-stage microstrip transformer and a small-signal microwave amplifier. We also perform yield sensitivity analysis for the three-stage microstrip transformer.

J.W. Bandler, R.M. Biernacki, S.H. Chen and P.A. Grobelny are with the Simulation Optimization Systems Research Laboratory, Department of Electrical and Computer Engineering, McMaster University, Hamilton, Canada L8S 4L7.

J.W. Bandler, R.M. Biernacki and S.H. Chen are also with Optimization Systems Associates Inc., P.O. Box 8083, Dundas, Ontario, Canada L9H 5E7.

S. Ye was with Optimization Systems Associates Inc., P.O. Box 8083, Dundas, Ontario, Canada L9H 5E7. He is now with Com Dev Ltd., Cambridge, Ontario, Canada N1R 7H6.

This work was supported in part by Optimization Systems Associates Inc. and in part by the Natural Sciences and Engineering Research Council of Canada under Grants OGP0007239, OGP0042444 and STR0117819 and through an Industrial Research Fellowship to S. Ye.

I. INTRODUCTION

A new multilevel multidimensional response surface modeling technique is presented for effective and efficient yield-driven design. This approach makes it possible, for the first time, to perform yield optimization as well as yield sensitivity analysis of circuits with microstrip structures simulated by an electromagnetic (EM) simulator.

Yield-driven design is now recognized as effective, not only for massively manufactured circuits but also to ensure first-pass success in any design where the prototype development is lengthy and expensive. The complexity of calculations involved in yield optimization requires special numerical techniques, e.g., [1-4]. In this paper we extend our previously published [2,4], highly efficient quadratic interpolation technique to dynamic multilevel response surface modeling. It has been specially designed to handle circuits containing complex subcircuits or components whose simulation requires significant computational effort.

With the increasing availability of EM simulators [5-7] it is very tempting to include them into performance-driven and even yield-driven circuit optimization. However, direct utilization of EM simulation for yield optimization or sensitivity analysis might seem to be computationally prohibitive. By constructing what we call local Q-models for each component simulated by an EM simulator we effectively overcome the computational burden of repeated EM simulations, which would otherwise be invoked for many statistical circuit outcomes throughout all yield optimization iterations. To maintain high accuracy, the Q-models are automatically updated whenever an outcome leaves the validity region of the current Q-model.

We show that when the proposed multilevel Q-modeling technique is used together with expensive, but more accurate simulations at the component level, the results are more reliable than those obtained from traditional analytical/empirical component simulations.

Efficiency and accuracy of our technique are demonstrated by yield optimization of a three-stage microstrip transformer and a small-signal amplifier. For the three-stage microstrip transformer we additionally perform yield sensitivity analyses and investigate different sets of optimization variables. Optimization was performed within the OSA90/hope™ [8] simulation-

optimization environment with Empipe™ [9] driving *em*™ [7] on a Sun SPARCstation 1+. We used the OSA90/hope one-sided ℓ_1 optimizer [10] for yield optimization.

II. EFFICIENT Q-MODELING

Formulation of the Method

The Q-model of a generic response $f(\boldsymbol{x})$, i.e., any response or gradient function for which we want to build and utilize the model, is a multidimensional quadratic polynomial of the form

$$q(\boldsymbol{x}) = a_0 + \sum_{i=1}^{n} a_i(x_i - r_i) + \sum_{\substack{i=1 \\ j \geq i}}^{n} a_{ij}(x_i - r_i)(x_j - r_j) \tag{1}$$

where $\boldsymbol{x} = [x_1\ x_2\ \ldots\ x_n]^T$ is the vector of generic parameters in terms of which the response is defined, and $\boldsymbol{r} = [r_1\ r_2\ \ldots\ r_n]^T$ is a chosen reference point in the parameter space.

To build the Q-model we use $n + 1 \leq m \leq 2n + 1$ base points at which the function $f(\boldsymbol{x})$ is evaluated. The reference point $\boldsymbol{r}$ is selected as the first base point $\boldsymbol{x}^1$. The remaining $m - 1$ base points are selected by perturbing one variable at a time around $\boldsymbol{r}$, namely,

$$\boldsymbol{x}^{i+1} = \boldsymbol{r} + [0\ \ldots\ 0\ \beta_i\ 0\ \ldots\ 0]^T,\quad i = 1, 2, \ldots, n \tag{2}$$

$$\boldsymbol{x}^{n+1+i} = \boldsymbol{r} + [0\ \ldots\ 0\ -\beta_i\ 0\ \ldots\ 0]^T,\quad i = 1, 2, \ldots, m - (n + 1) \tag{3}$$

where β_i is a predetermined perturbation. If a variable is perturbed twice the second perturbation is located symmetrically w.r.t. $\boldsymbol{r}$. We have applied the Maximally Flat Quadratic Interpolation (MFQI) technique [2] to such a set of base points (see [3, 4] for details). MFQI builds the Q-model by minimizing in the least-squares sense all the second-order term coefficients in (1). It is intuitively equivalent to constructing an interpolation which has the smallest deviation from the linear interpolation.

Implementation

Applying MFQI to the base points defined by $\boldsymbol{r}$, (2) and (3) and reordering the variables such that the first $m - (n + 1)$ variables are perturbed twice yields the following formulas for the coefficients in (1)

$$a_{ii} = \frac{1}{2\beta_i^2}[f(\boldsymbol{x}^{n+1+i}) + f(\boldsymbol{x}^{i+1}) - 2f(\boldsymbol{r})], \quad i = 1, 2, \ldots, m - (n + 1) \tag{4a}$$

$$a_{ii} = 0, \quad i = m - n, \ldots, n, \quad m \neq 2n + 1 \tag{4b}$$

and

$$a_{ij} = 0, \quad i, j = 1, 2, \ldots, n, \quad i \neq j \tag{4c}$$

The coefficients a_0 and a_i are given by

$$a_0 = f(\boldsymbol{r}) \tag{5}$$

$$a_i = \frac{1}{2\beta_i}[-f(\boldsymbol{x}^{n+1+i}) + f(\boldsymbol{x}^{i+1})], \quad i = 1, 2, \ldots, m - (n + 1) \tag{6a}$$

and

$$a_i = \frac{1}{\beta_i}[f(\boldsymbol{x}^{i+1}) - f(\boldsymbol{r})], \quad i = m - n, \ldots, n, \quad m \neq 2n + 1 \tag{6b}$$

Substituting (4), (5) and (6) into (1) results in the following formula for the Q-model $q(\boldsymbol{x})$

$$q(\boldsymbol{x}) = f(\boldsymbol{r}) + \sum_{i=1}^{m-(n+1)} \left\{[f(\boldsymbol{x}^{i+1}) - f(\boldsymbol{x}^{n+1+i}) + (f(\boldsymbol{x}^{i+1}) + f(\boldsymbol{x}^{n+1+i}) - 2f(\boldsymbol{r}))(x_i - r_i)/\beta_i](x_i - r_i)/(2\beta_i)\right\}$$

$$+ \sum_{i=m-n}^{n} \left\{[f(\boldsymbol{x}^{i+1}) - f(\boldsymbol{r})](x_i - r_i)/\beta_i\right\} \tag{7}$$

It is important to realize that the variable number of base points m offers a trade-off between the accuracy and cost of circuit analysis. Reducing the number of base points decreases

the number of function evaluations. However, perturbing a variable only once results in a linear rather then quadratic interpolation w.r.t. that variable. This provides a spectrum of available models from a linear model L-model, for $m = n + 1$, to a quadratic model w.r.t. all variables for $m = 2n + 1$.

The simplicity of (7) results in high efficiency of the approach. It should be noted that the computational effort increases only linearly with the number of variables n.

To apply a gradient-based optimizer we need to provide the gradient of functions $q(\boldsymbol{x})$ which are actually used by the optimizer. Differentiating (7) w.r.t. x_i results in

$$\partial q(\boldsymbol{x})/\partial x_i = [(f(\boldsymbol{x}^{i+1}) - f(\boldsymbol{x}^{n+1+i}))/2 + (f(\boldsymbol{x}^{i+1}) + f(\boldsymbol{x}^{n+1+i}) - 2f(\boldsymbol{r}))(x_i - r_i)/\beta_i]/\beta_i, \quad i = 1, \ldots, m - (n + 1) \tag{8a}$$

and

$$\partial q(\boldsymbol{x})/\partial x_i = [f(\boldsymbol{x}^{i+1}) - f(\boldsymbol{r})]/\beta_i, \quad i = m - n, \ldots, n, \quad m \neq 2n + 1 \tag{8b}$$

which again is very efficient.

Linear Versus Quadratic Modeling

We use a simple example in which we approximate the response of a microstrip line simulated as a two port network by the ***em*** [7] simulator.

We fix the width of the microstrip line and sweep its length l with a step Δl. First, we simulate the circuit at each point in the sweep. This provides us with the response reference data. Subsequently, we use both L- and Q-models to approximate responses at *every other* sweep point using adjacent sweep points as the model base points. Fig. 1 summarizes the results. It shows the real part of S_{11} with l swept from 3.2 to 3.8 mm and $\Delta l = 0.1$ mm. The responses for $l = 3.3$, 3.5 and 3.7 mm are modeled. The L-model uses responses at two adjacent points to model the response at the point in between, e.g., responses at points 3.2 and 3.4 mm are used to model the response at 3.3 mm. The Q-model uses three points, e.g., responses at points 3.4, 3.6 and 3.8 mm are used to model the response at 3.7 mm.

It can be seen that the Q-model is more accurate than the L-model.

III. MULTILEVEL SIMULATION AND MODELING

Multilevel Modeling

Multilevel modeling is depicted schematically in Fig. 2. The circuit under consideration is divided into subcircuits, possibly in a hierarchical manner. At the lowest level we have circuit components, e.g., a lumped capacitor or a microstrip structure.

Defining f_c, f_s and f_e as circuit, subcircuit and component responses, respectively, we can express the response of the circuit as a function of the subcircuit responses which are in turn functions of component responses. This hierarchy can be expressed formally as

$$f_c = f_c(f_{s1}, f_{s2}, \ldots, f_{sn_s}) \tag{9}$$

$$f_{si} = f_{si}(f_{ei1}, f_{ei2}, \ldots, f_{ein_{ei}}), \quad i = 1, 2, \ldots, n_s \tag{10}$$

and

$$f_{eij} = f_{eij}(\boldsymbol{x}), \quad i = 1, 2, \ldots, n_s, \quad j = 1, 2, \ldots, n_{ei} \tag{11}$$

where n_s is the number of subcircuits and n_{ei} is the number of components in the ith subcircuit. $\boldsymbol{x}$ is the vector of circuit parameters. The responses are typically frequency-domain functions of multiport responses.

We can create a single Q-model for the overall circuit. We can also create a hierarchy of Q-models to represent some or all of the subcircuits and components, as illustrated in Fig. 2.

If, for example, the vector of base points of a Q-model is given as $[\boldsymbol{x}^1\ \boldsymbol{x}^2\ \ldots\ \boldsymbol{x}^m]^T$, where $\boldsymbol{x}^1$ is treated as the reference point $\boldsymbol{r}$ (see (2) and (3)) and $n + 1 \le m \le 2n + 1$, with n being the number of model parameters, then we can express the simulation results at these base points as

$$[f(\boldsymbol{x}^1)\ f(\boldsymbol{x}^2)\ \ldots\ f(\boldsymbol{x}^m)] \tag{12}$$

with

$$f(\boldsymbol{x}^i) = [f_1(\boldsymbol{x}^i)\ f_2(\boldsymbol{x}^i)\ \ldots\ f_k(\boldsymbol{x}^i)]^T, \quad i = 1, 2, \ldots, m \tag{13}$$

where k is the total number of different responses. f can be a response of either circuit, subcircuit or a component. Then

$$f(\boldsymbol{x}) \approx \boldsymbol{q}(\boldsymbol{x}) = [q_1(\boldsymbol{x})\ q_2(\boldsymbol{x})\ \ldots\ q_k(\boldsymbol{x})]^T \tag{14}$$

The Q-models in (14) approximate $f(\boldsymbol{x})$ for $\boldsymbol{x}$ belonging to the Q-model validity region centered around the reference point $\boldsymbol{r} = \boldsymbol{x}^1$.

Implementation

During optimization the design center moves, and so does the set of associated statistical outcomes. This may result in moving some or even all of the statistical outcomes out of the validity region of the current Q-models. In the present implementation the validity region $\boldsymbol{V}$ is defined as

$$\boldsymbol{V} = \{\boldsymbol{x} \mid (x_i - r_i) \le \beta_i/2,\ (r_i - x_i) < \beta_i/2\},\quad i = 1, 2, \ldots, n \tag{15}$$

where β_i is the perturbation used in (2) and (3) to compute the model base points. Moving a point outside the current $\boldsymbol{V}$ requires that the Q-models in (14), and hence $\boldsymbol{V}$, be appropriately updated. We have developed an updating scheme in which the Q-models are updated automatically in real optimization time. If a statistical outcome is outside the current $\boldsymbol{V}$, a new set of base points is generated and the responses at these base points are simulated *but only if they have not been simulated previously*. Updated Q-models follow immediately from recomputing (7). Our Q-model updating scheme is based on a data base system storing results for newly simulated base points and providing extremely fast access to the results of already simulated base points. The data base and Q-models are updated whenever new results become available.

If all components, subcircuits and the overall circuit were to be simulated rather than modeled the evaluation of the circuit response f_c could proceed as follows.

```
for the ith subcircuit, i = 1, 2, ..., n_s {
        for the jth component in the ith subcircuit, j = 1, 2, ..., n_ei {
                find f_eij by simulating the component according to (11);
        }
        find f_si according to (10);
}
find f_c according to (9);
```

Applying this algorithm to yield estimation or optimization may become prohibitive, especially if an EM simulator is to be used. Replacing costly circuit simulations with model evaluations yields an alternative algorithm.

```
if circuit model q_c exists
        evaluate q_c;
else {
        for the ith subcircuit, i = 1, 2, ..., n_s {
                if subcircuit model q_si exists {
                        evaluate q_si;
                }
                else {
                        for the jth component in the ith subcircuit, j = 1, 2, ..., n_ei {
                                if component model q_eij exists {
                                        evaluate q_eij;
                                }
                                else {
                                        find f_eij by simulating the component according to (11);
                                }
                        }
                        find f_si according to (11);
                }
        }
        find f_c according to (9);
}
```

Here, some of the responses f_{eij}, f_{si} or f_c are replaced by the corresponding models q_{eij}, q_{si} or q_c.

Discrete Parameters

The circuit, subcircuits and components may contain discrete parameters. For discrete parameters simulation can only be performed at discrete values located on the grid, as illustrated in Fig. 3. Normally, the reference vector $\boldsymbol{r}$ is taken as the nominal point $\boldsymbol{x}^1$. This is likely to be off-the-grid. Similarly, the other base points $\boldsymbol{x}^{i+1}$ and $\boldsymbol{x}^{n+1+i}$ are likely to be off-the-grid. Local

interpolation involving several simulations on the grid in the vicinity of each of the base points must then be performed. In order to avoid these excessive simulations those base points are modified to snap to the grid.

IV. YIELD OPTIMIZATION OF A 3-SECTION MICROSTRIP TRANSFORMER

The Transformer

A 3-section 3:1 microstrip impedance transformer is shown in Fig. 4. The source and load impedances are 50 and 150 ohms, respectively. The design specification is set for input reflection coefficient as

$$|S_{11}| \leq 0.12, \text{ from 5 GHz to 15 GHz}$$

The error functions for yield optimization are calculated for frequencies from 5 GHz to 15 GHz with a 0.5 GHz step. The transformer is built on a 0.635 mm thick substrate with relative dielectric constant 9.7.

For EM simulators, the circuit is typically partitioned into components which are defined to encompass parts of the structure that can be isolated from the other parts. This can significantly increase the efficiency of EM simulation.

The transformer was decomposed into three components, each corresponding to a different section of the transformer. In order to account for the discontinuity effects the first two sections were simulated as step discontinuities and the last section as a microstrip line. Each of the components is simulated as a two-port network.

As a verification, we also simulated the entire transformer structure as one piece. The results of simulating the circuit at the nominal minimax solution using the two methods are virtually the same.

Yield Optimization with Six Optimization Variables

We start yield optimization from the solution of a nominal design with W_1, W_2, W_3, L_1, L_2 and L_3 as variables. Normal distributions with 2% standard deviations were assumed for W_1, W_2

and W_3 and 1% standard deviations for L_1, L_2 and L_3. Three component level Q-models were established for each section of the transformer at the nominal point using ***em*** [7]. The Q-models were updated during the optimization process whenever necessary.

Utilizing these Q-models we conducted two experiments to demonstrate multilevel Q-modeling: (1) yield optimization using single-level (component) modeling, and (2) yield optimization using two-level (component and circuit response) modeling. 100 statistical outcomes were used for yield optimization. The solutions in both cases are almost identical: yield (estimated by 250 outcomes) is increased from 71% to 86% using single-level modeling and to 85% using two-level modeling. Fig. 5(a) illustrates the Monte Carlo sweep before optimization and Fig. 5(b) shows the corresponding sweep after yield optimization using single-level (component) modeling. The values of the optimization variables before and after yield optimization for both single- and two-level modeling are given in Table I. The solution of design centering is quite close to the nominal minimax design. This is expected, taking into account small tolerances on the parameters.

CPU time for yield optimization, performed on a Sun SPARCstation 1+, was 16 minutes for single-level modeling and 3 minutes when multilevel Q-models were used. Elapsed time for the ***em*** [7] simulations using single-level modeling was about 100 hours. The two-level modeling approach exploited the data base created during single-level optimization and did not require any additional ***em*** [7] simulations.

Yield Optimization with Three Optimization Variables

We investigated yield optimization with W_1, W_2 and W_3 as variables. L_1, L_2 and L_3 were not optimized. The solutions obtained using component and both component and circuit modeling are again very similar. Yield is increased to 79% with component-level Q-models and to 78% with component- and circuit-level Q-models. Parameter values for both solutions are listed in Table II. The CPU time was 5 minutes for component-level and 41 seconds for two-level Q-modeling. The previously established data base was sufficient for this experiment, so that no additional ***em*** [7] simulations were required.

Yield Sensitivity Analysis

We performed the yield sensitivity analysis at the centered solution obtained using six optimization variables. Fig. 6 shows yield as a function of the specification. The specification is swept from 0.10 to 0.13 with 0.005 step using 250 Monte Carlo outcomes. The diagram confirms high sensitivity of yield w.r.t. the specification. The yield varies from 0% to 100% over a very small range of the specification.

We performed sensitivity analysis w.r.t. all six optimization variables using 250 statistical outcomes. As expected, the yield is very sensitive to the widths of all the sections and it is insensitive to the lengths of the sections. We also observed that the yield exhibits highest sensitivity w.r.t the width of the third section W_3. The analysis required very little additional computational effort. See Fig. 7 for the results.

V. YIELD OPTIMIZATION OF A SMALL-SIGNAL AMPLIFIER

The specification for a typical single-stage 6-18 GHz small-signal amplifier shown in Fig. 8 is

$$7 \text{ dB} \leq |S_{21}| \leq 8 \text{ dB}, \text{ from 6 GHz to 18 GHz}$$

The error functions for yield optimization are calculated at frequencies from 6 GHz to 18 GHz with a 1 GHz step. The gate and drain circuit microstrip T-junctions and the feedback microstrip line are built on a 10 mil thick substrate with relative dielectric constant 9.9.

First, we performed nominal minimax optimization using analytical/empirical microstrip component models. W_{g1}, L_{g1}, W_{g2}, L_{g2} of the gate circuit T-junction and W_{d1}, L_{d1}, W_{d2}, L_{d2} of the drain circuit T-junction were selected as optimization variables. W_{g3}, L_{g3}, W_{d3} and L_{d3} of the T-junctions, W and L of the feedback microstrip line, as well as the FET parameters were not optimized. Fig. 9 shows the parameters of the T-junctions and the microstrip line. Fig. 10 shows the small-signal FET model.

We assumed a 0.5 mil tolerance and uniform distribution for all geometrical parameters of the microstrip components. The statistics of the small-signal FET model were extracted from measurement data [11] and are given in Table III. The correlations among FET model parameters are listed in Table IV. The value of the feedback resistor was 1600 ohms.

Monte Carlo simulation with 250 outcomes performed at the nominal solution with analytical/empirical microstrip component models reported 91% yield. To obtain a more accurate estimate, we used component level Q-models built from *em* [7] simulations for the microstrip components. The yield dropped to 55%. Figs. 11(a) and 11(b) show the Monte Carlo sweeps obtained using analytical/empirical and our *em* [7] based Q-models, respectively. Close similarities can be observed for lower frequencies, while discrepancies become larger for higher frequencies.

Utilizing the component level quadratic Q-models built from *em* simulations, we further performed yield optimization of this amplifier. Yield estimated by 250 Monte Carlo simulations was increased to 82%. The corresponding Monte Carlo sweep diagram is shown in Fig. 12. Yield and the values of the optimization variables before and after optimization are given in Table V.

VI. CONCLUSIONS

We have presented a new multilevel quadratic modeling technique suitable for effective and efficient yield-driven design optimization. The method dynamically integrates the Q-models and data base generation and updating, increasing both speed of processing and accuracy of the results. The approach is particularly useful for circuits containing complex subcircuits or components whose simulation requires significant computational effort. The efficiency of this technique allowed us to perform yield-driven design and to analyze yield sensitivity for circuits containing microstrip structures accurately simulated by *em* [7]. We used a three-stage microstrip transformer and a small-signal amplifier to demonstrate the efficiency and accuracy of the method. Our approach significantly extends the microwave CAD applicability of yield optimization techniques.

ACKNOWLEDGEMENT

The authors thank Dr. J.C. Rautio of Sonnet Software, Inc., Liverpool, NY for his initiatives and making ***em*** available for this work.

REFERENCES

[1] J.W. Bandler and S.H. Chen, "Circuit optimization: the state of the art," *IEEE Trans. Microwave Theory Tech.*, vol. 36, 1988, pp. 424-443.

[2] R.M. Biernacki and M.A. Styblinski, "Efficient performance function interpolation scheme and its application to statistical circuit design," *IEEE Int. J. Circuit Theory and Appl.*, vol. 19, 1991, pp. 403-422.

[3] R.M. Biernacki, J.W. Bandler, J. Song and Q.J. Zhang, "Efficient quadratic approximation for statistical design," *IEEE Trans. Circuit Syst.*, vol. 36, 1989, pp. 1449-1454.

[4] J.W. Bandler, R.M. Biernacki, S.H. Chen, J. Song, S. Ye and Q.J. Zhang, "Gradient quadratic approximation scheme for yield-driven design," *IEEE MTT-S Int. Microwave Symp. Dig.* (Boston, MA), 1991, pp. 1197-1200.

[5] T. Itoh, Ed., *Numerical Techniques for Microwave and Millimeter-Wave Passive Structures.* New York: Wiley, 1989.

[6] R.H. Jansen and P. Pogatzki, "A hierarchically structured, comprehensive CAD system for field theory-based linear and nonlinear MIC/MMIC design," *1992 2nd Int. Workshop of the German IEEE MTT/AP Joint Chapter on Integrated Nonlinear Microwave and Millimeterwave Circuits Dig.* (Duisburg, Germany), 1992, pp. 333-341.

[7] *Em User's Manual* and *Xgeom User's Manual*, Sonnet Software, Inc., 135 Old Cove Road, Suite 203, Liverpool, NY 13090-3774, May 1992.

[8] *OSA90/hope™ Version 2.0 User's Manual*, Optimization Systems Associates Inc., P.O. Box 8083, Dundas, Ontario, Canada L9H 5E7, 1992.

[9] *Empipe™ Version 1.0 Technical Brief*, Optimization Systems Associates Inc., P.O. Box 8083, Dundas, Ontario, Canada L9H 5E7, 1992.

[10] J.W. Bandler, S.H. Chen and K. Madsen, "An algorithm for one-sided ℓ_1 optimization with application to circuit design centering," *Proc. IEEE Int. Symp. Circuits Syst.* (Espoo Finland), 1988, pp. 1795-1798.

[11] Measurement data provided by Plessey Research Caswell Ltd., Caswell, Towcester, Northamptonshire, England NN12 8EQ, 1990.

TABLE I
MICROSTRIP PARAMETERS OF THE 3-SECTION MICROSTRIP TRANSFORMER

Parameters	Nominal design	Centered design (single-level modeling)	Centered design (two-level modeling)
W_1	0.4294	0.4363	0.4377
W_2	0.2080	0.2055	0.2053
W_3	0.07	0.07	0.07
L_1	3.0	2.951	2.8875
L_2	3.0	2.998	3.0007
L_3	3.0	3.046	3.058
Yield (250 outcomes)	71%	86%	85%

Dimensions of the parameters are in millimeters. 100 outcomes were used for yield optimization.

TABLE II
MICROSTRIP PARAMETERS OF THE 3-SECTION MICROSTRIP TRANSFORMER

Parameters	Nominal design	Centered design (single-level modeling)	Centered design (two-level modeling)
W_1	0.4294	0.4339	0.4333
W_2	0.2080	0.2081	0.2079
W_3	0.07	0.07	0.07
L_1	3.0*	3.0*	3.0*
L_2	3.0*	3.0*	3.0*
L_3	3.0*	3.0*	3.0*
Yield (250 outcomes)	71%	79%	78%

* Parameters not optimized.

Dimensions of the parameters are in millimeters. 100 outcomes were used for yield optimization.

TABLE III
EXTRACTED STATISTICAL DISTRIBUTIONS FOR THE FET PARAMETERS (FIG. 10)

FET Parameter	Mean Value	Standard Deviation (%)	FET Parameter	Mean Value	Standard Deviation (%)
$R_G(\Omega)$	2.035	3	C_{DS}(pF)	0.06978	1
$R_D(\Omega)$	3.421	8	g_m	-0.0713	2
$R_S(\Omega)$	3.754	6	τ(pS)	1.9093	2
L_S(nH)	0.0811	7	C_{GD}(pF)	0.02606	2
$G_{DS}(1/\Omega)$	0.00598	1	C_{GS}(pF)	0.30319	1.5

TABLE IV
EXTRACTED FET MODEL PARAMETER CORRELATIONS

	R_G	R_D	R_S	L_S	G_{DS}	C_{DS}	g_m	τ	C_{GD}	C_{GS}
R_G	1	-0.3121	-0.5869	0.5244	0.1914	-0.1805	-0.4473	-0.0567	-0.0971	-0.2548
R_D	-0.3121	1	0.7279	-0.7479	0.07056	0.411	0.3914	-0.047	-0.206	0.2474
R_S	-0.5869	0.7279	1	-0.8461	-0.0663	0.4825	0.6637	-0.2376	-0.1262	0.1974
L_S	0.5244	-0.7479	-0.8461	1	0.0162	-0.7326	-0.5204	0.02553	0.3676	-0.3084
G_{DS}	0.1914	0.07056	-0.0663	0.0162	1	0.1504	-0.5752	-0.2991	-0.171	0.3561
C_{DS}	-0.1805	0.411	0.4825	-0.7326	0.1504	1	0.1765	0.0295	-0.6786	0.1946
g_m	-0.4473	0.3914	0.6637	-0.5204	-0.5752	0.1765	1	-0.1781	0.0863	-0.3412
τ	-0.0567	-0.047	-0.2376	0.02553	-0.2991	0.0295	-0.1781	1	-0.2122	0.2624
C_{GD}	-0.0971	-0.206	-0.1262	0.3676	-0.171	-0.6786	0.0863	-0.2122	1	-0.2904
C_{GS}	-0.2548	0.2474	0.1974	-0.3084	0.3561	0.1946	-0.3412	0.2624	-0.2904	1

TABLE V
MICROSTRIP PARAMETERS OF THE AMPLIFIER

Parameters	Nominal design	Centered design
W_{g1}	17.45	19
L_{g1}	35.54	34.53
W_{g2}	9.01	8.611
L_{g2}	30.97	32
W_{g3}	3*	3*
L_{g3}	107*	107*
W_{d1}	8.562	7
L_{d1}	4.668	6
W_{d2}	3.926	3.628
L_{d2}	9.902	11
W_{d3}	3.5*	3.5*
L_{d3}	50*	50*
W	2*	2*
L	10*	10*
Yield (250 outcomes)	55%	82%

* Parameters not optimized.

Dimensions of the parameters are in mils. 50 outcomes were used for yield optimization. 0.5 mil tolerance and uniform distribution were assumed for all the parameters.

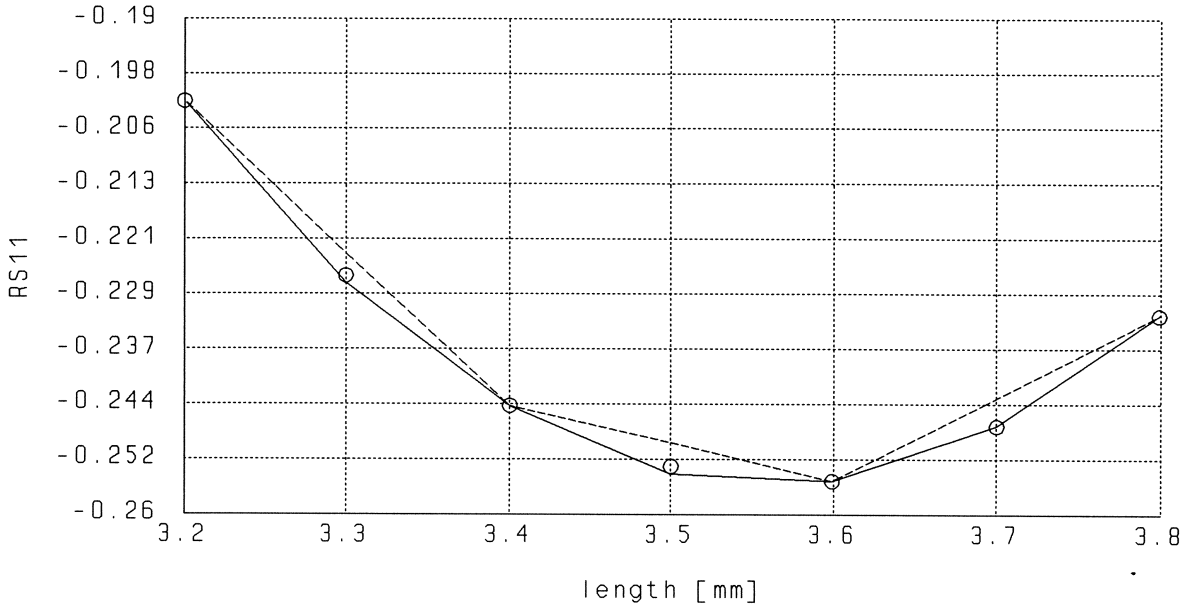

Fig. 1 Comparison between linear (---) and quadratic (——) approximations of the real part of S_{11} of a microstrip line simulated by the ***em*** [7] simulator (O).

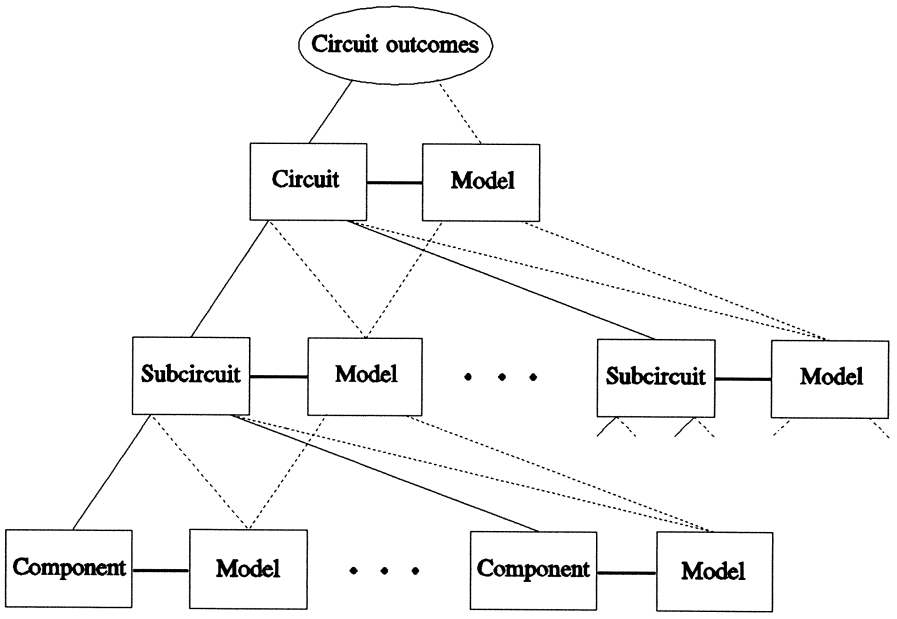

Fig. 2 Schematic diagram illustrating multilevel modeling for yield-driven optimization. Solid and dotted lines distinguish between simulated and modeled responses.

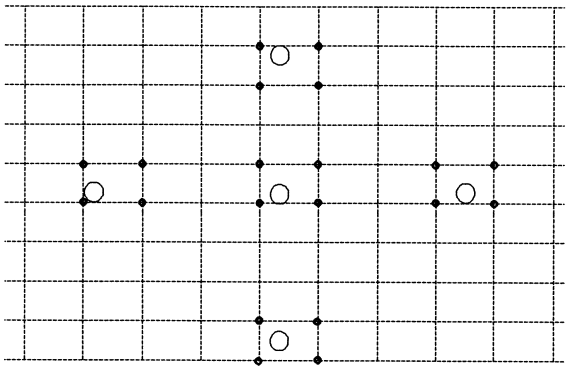

Fig. 3 Illustration of base points and discrete points. The large circles represent possible locations of base points w.r.t. a grid. The solid dots indicate discrete simulation points on the grid. If the base points are snapped to the grid, the number of simulations can be significantly reduced.

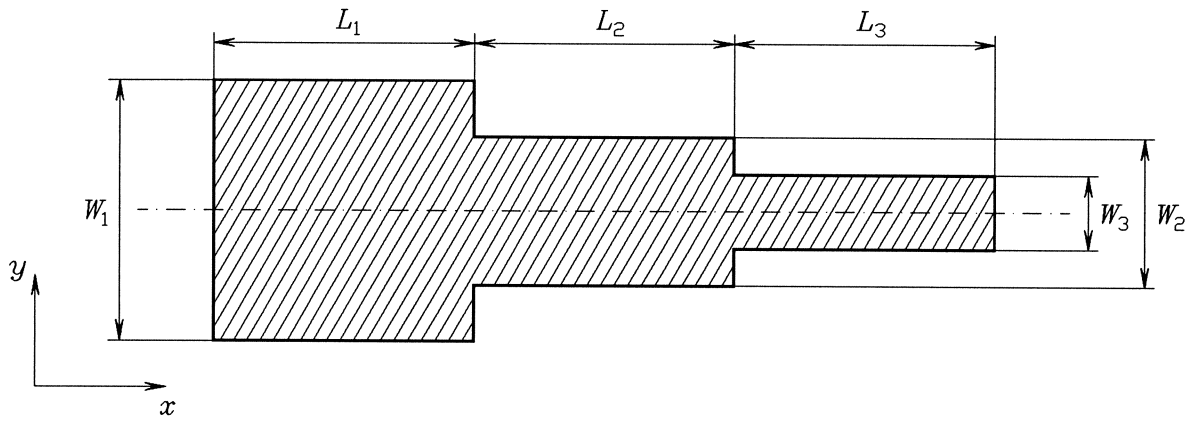

Fig. 4 The 3-section 3:1 microstrip impedance transformer. The thickness and dielectric constant of the substrate are 0.635 mm and 9.7, respectively.

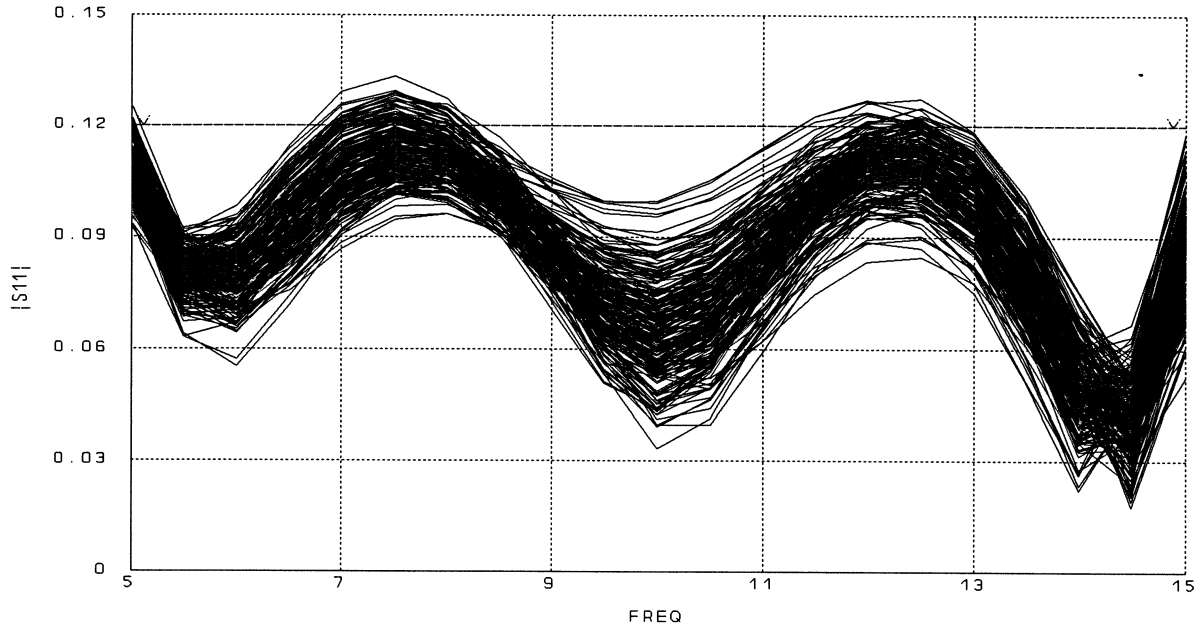

(a)

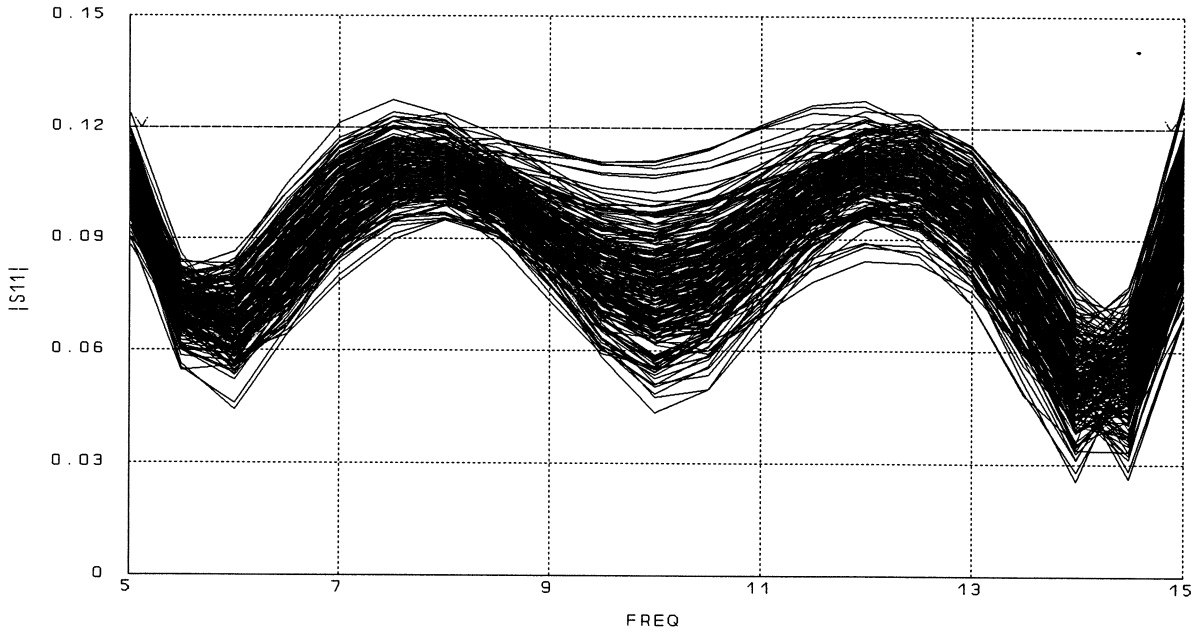

(b)

Fig. 5 Modulus of the reflection coefficient of the 3-section microstrip impedance transformer vs. frequency: (a) before and (b) after yield optimization. Yield is increased from 71% to 86% after optimization using single-level (component) Q-models.

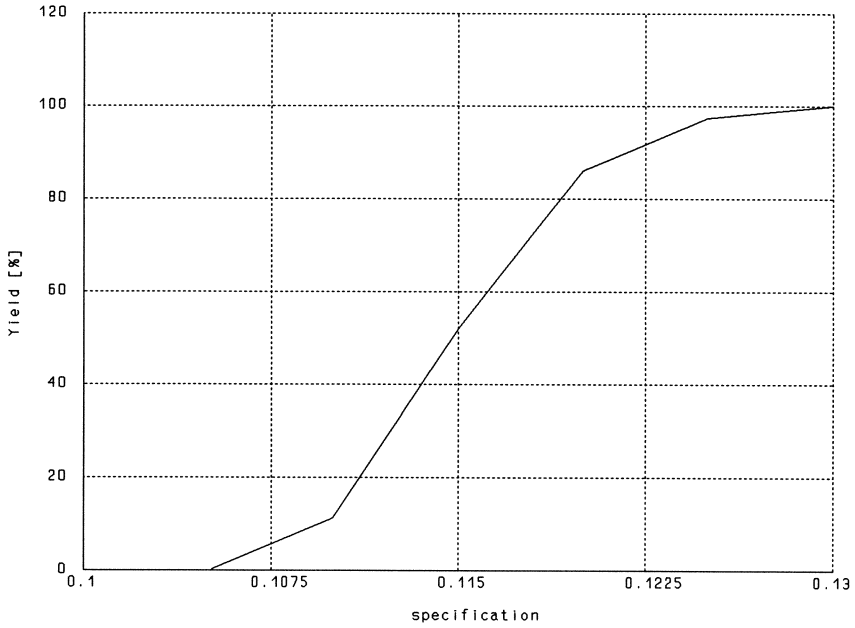

Fig. 6 Yield of the three-section microstrip transformer as a function of the specification imposed on $|S_{11}|$. High sensitivity of yield w.r.t. the specification can be observed. Yield is estimated with 250 Monte Carlo outcomes.

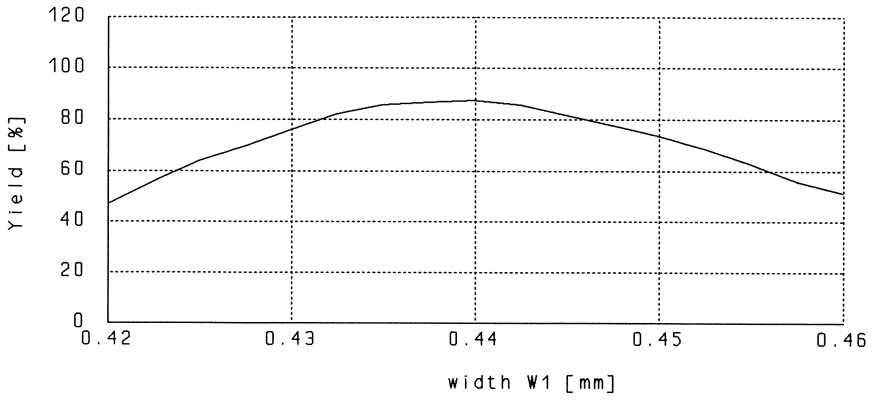

(a)

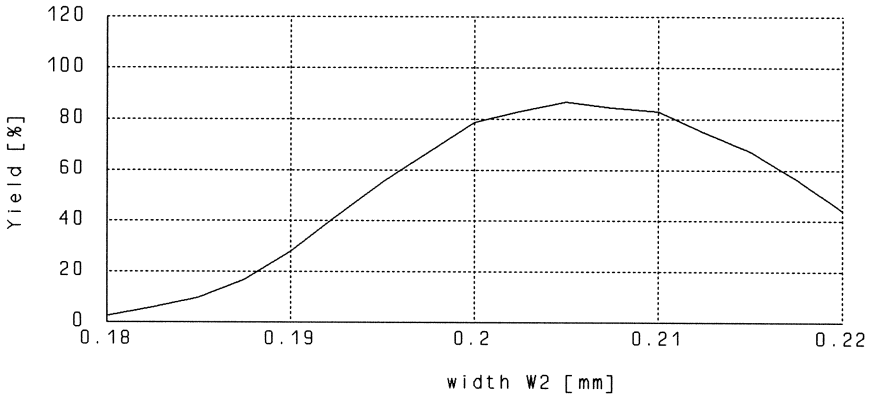

(b)

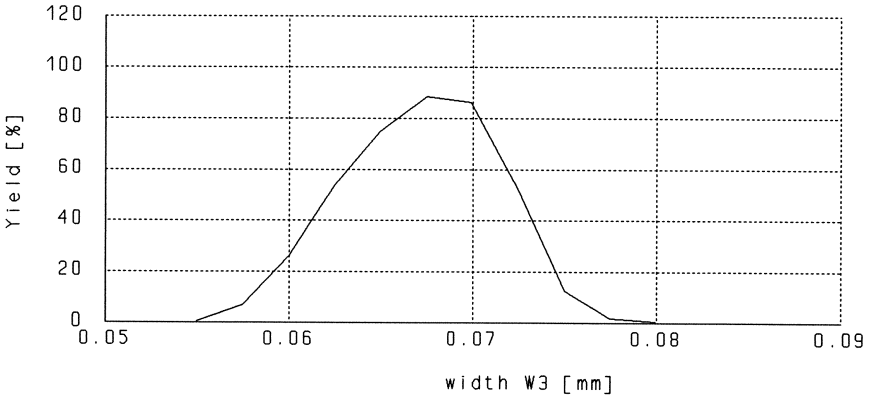

(c)

Fig. 7 Yield sensitivity analysis for the three-stage microstrip transformer at the centered solution. 250 Monte Carlo outcomes were used for yield estimation. The results are obtained with little additional computational effort. Yield as a function of (a) W_1, (b) W_2 and (c) W_3.

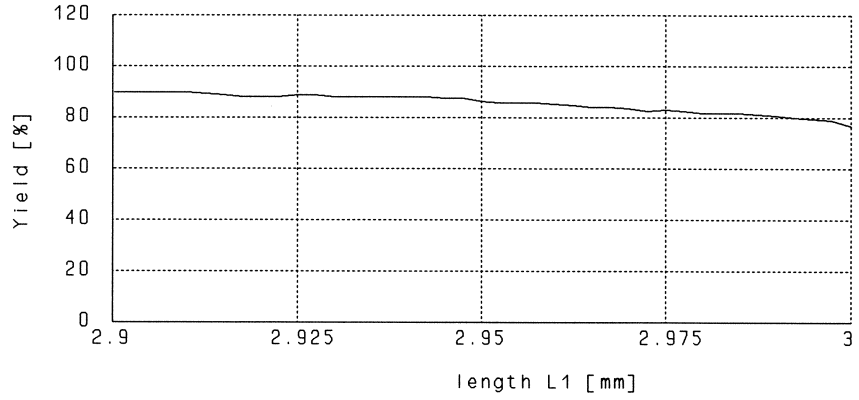

(d)

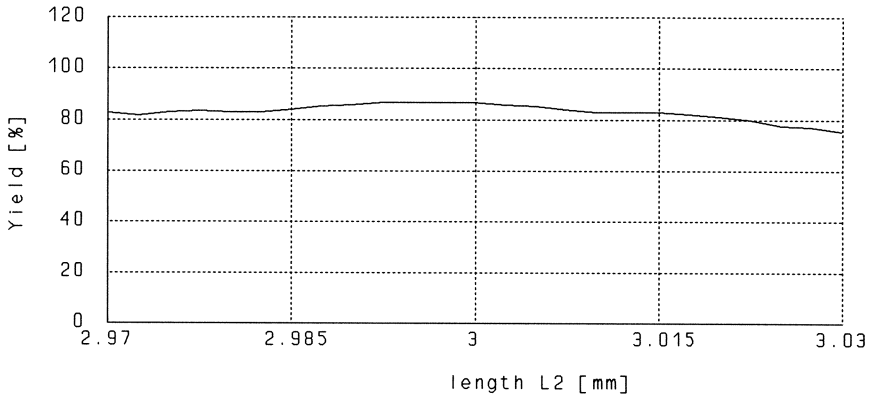

(e)

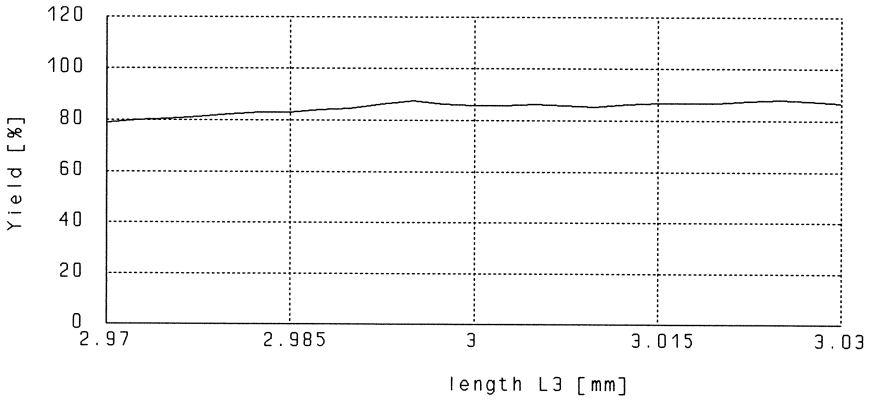

(f)

Fig. 7 (con'd) Yield as a function of (d) L_1, (e) L_2 and (f) L_3.

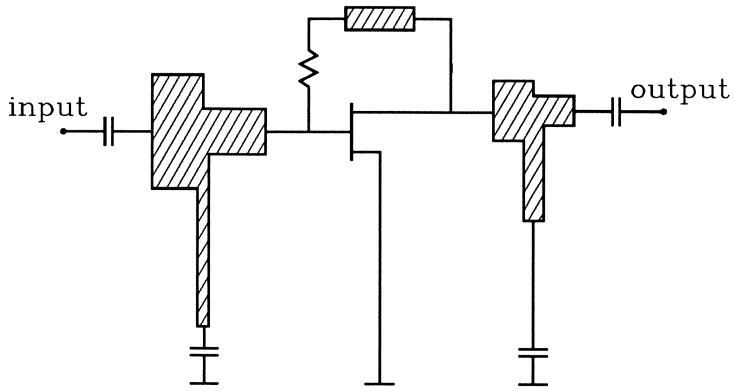

Fig. 8 Circuit diagram of the 6-18 GHz small-signal amplifier. We use ***em*** [7] to model the two T-junctions and the microstrip line.

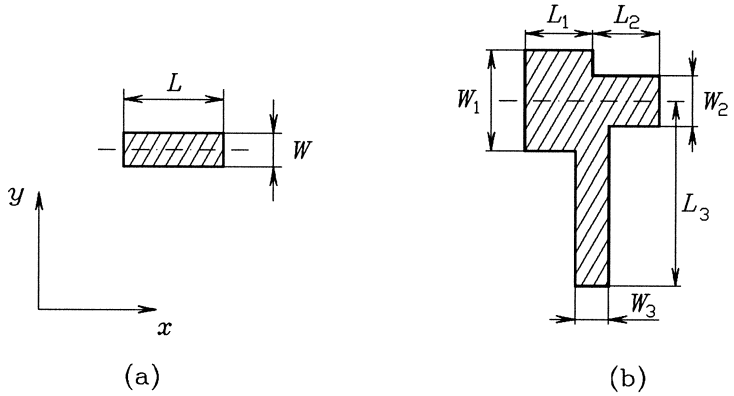

Fig. 9 Parameters of (a) the feedback microstrip line and (b) the microstrip T-junctions.

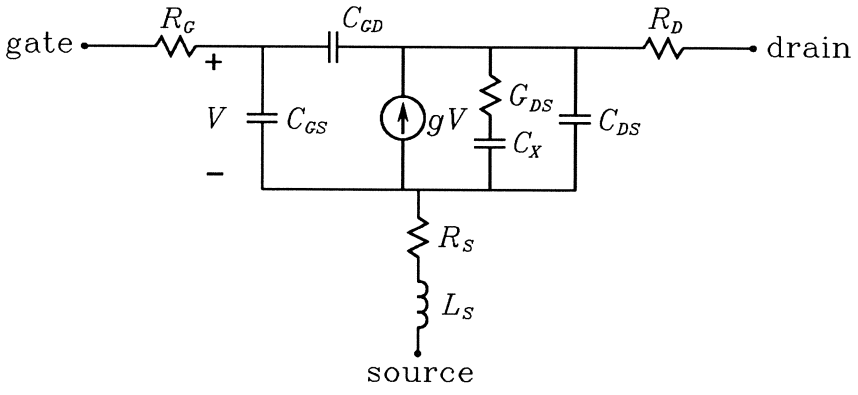

Fig. 10 Schematic diagram of the small-signal FET model. The value of the capacitor C_x is 2.0 pF. The transadmitance g is evaluated as $g = g_m e^{-2j\pi f\tau}$, where g_m and τ are given in Table III and f is the frequency.

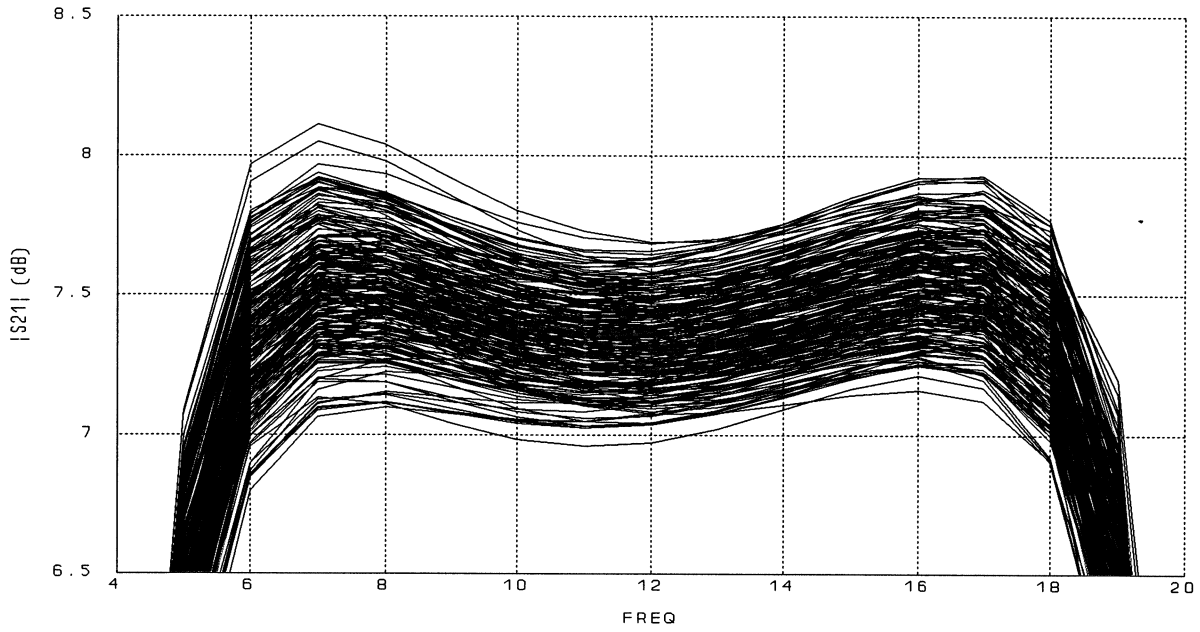

(a)

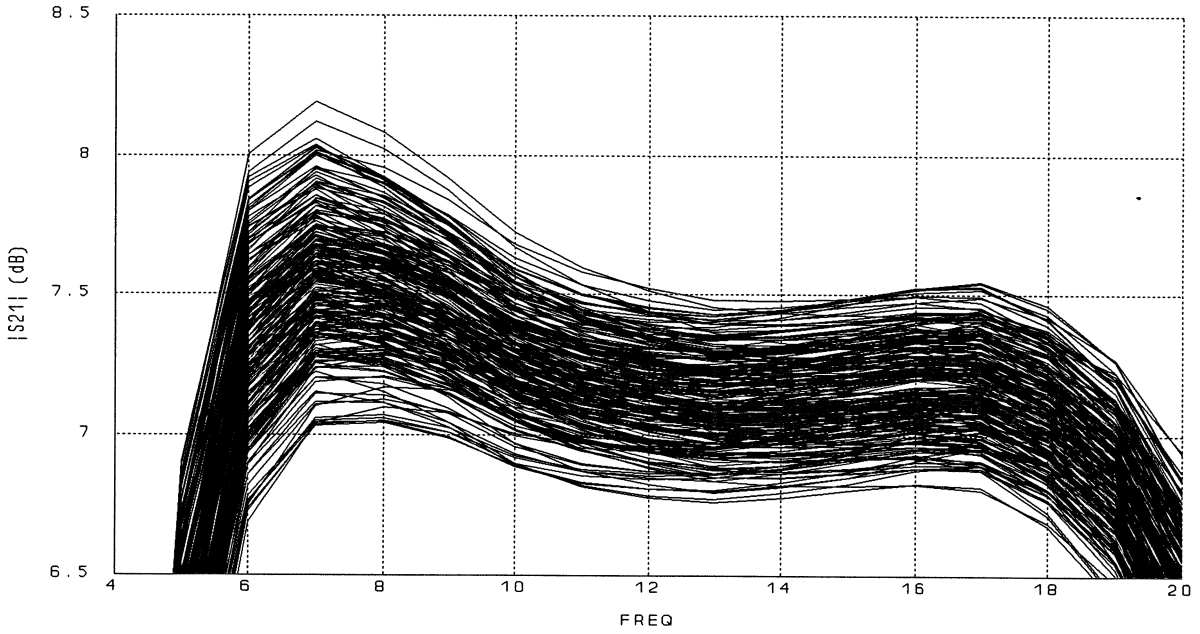

(b)

Fig. 11 $|S_{21}|$ of the small-signal amplifier for 250 statistical outcomes at the nominal minimax solution: (a) using analytical/empirical microstrip component models, and (b) using ***em*** [7] based Q-models.

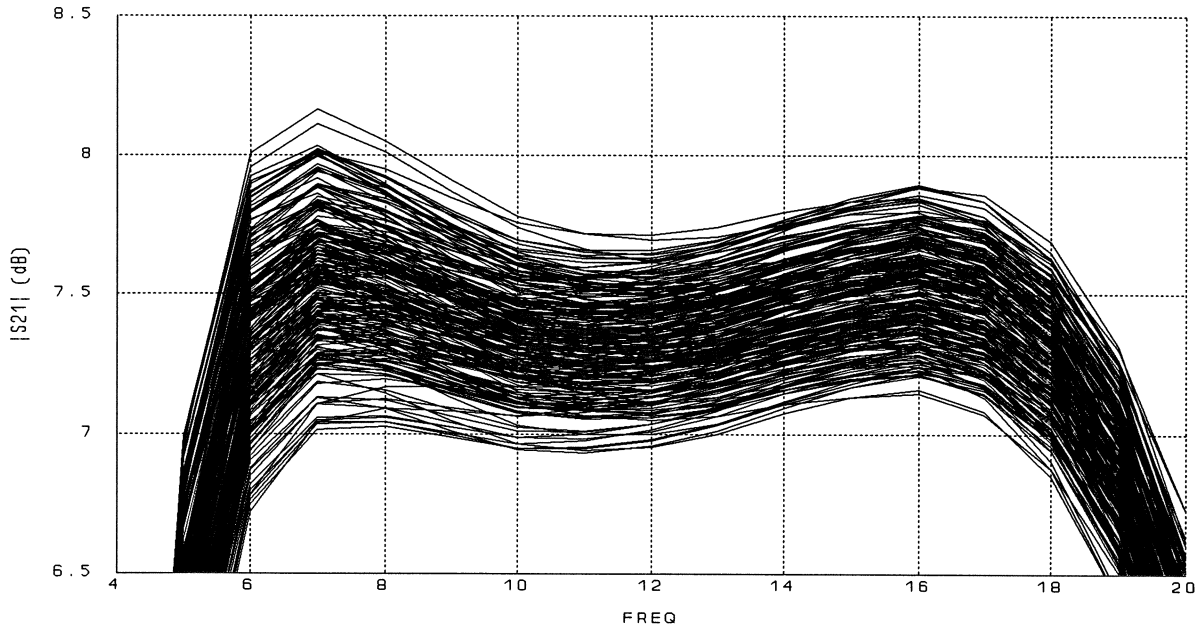

Fig. 12 $|S_{21}|$ of the small-signal amplifier for 250 statistical outcomes after yield optimization using *em* [7] based Q-models. Yield is increased from 55% to 82%.